ISSN 1674-1056
http://cpb.iphy.ac.cn
http://iopscience.iop.org/cpb
中国物理 B
Chinese Physics
中国物理
Chinese Physics B

Numerical study of heat-transfer in two- and quasi-two-dimensional Rayleigh-Bénard convection

Zhen-Yuan Gao(高振源), Jia-Hui Luo(罗嘉辉), Yun Bao(包芸)

Citation: Chin. Phys. B . 2018, 27(10): 104702. **doi:** 10.1088/1674-1056/27/10/104702

Journal homepage: http://cpb.iphy.ac.cn; http://iopscience.iop.org/cpb

What follows is a list of articles you may be interested in

Turbulence modulation model for gas-particle flow based on probability density function approach

Lu Wang(王路), Jiang-rong Xu(徐江荣)

Chin. Phys. B . 2017, 26(8): 084702. **doi:** 10.1088/1674-1056/26/8/084702

Characteristics and generation of elastic turbulence in a three-dimensional parallel plate channel using direct numerical simulation

Hong-Na Zhang(张红娜), Feng-Chen Li(李凤臣), Xiao-Bin Li(李小斌), Dong-Yang Li(李东阳), Wei-Hua Cai(蔡伟华), Bo Yu(宇波)

Chin. Phys. B . 2016, 25(9): 094701. **doi:** 10.1088/1674-1056/25/9/094701

Effect of noncircular orifice plates on the near flow field of turbulent free jets

Xu Min-Yi, Tong Xing-Qing, Yue Dan-Ting, Zhang Jian-Peng, Mi Jian-Chun, Nathan G. J., Kalt P. A. M.

Chin. Phys. B . 2014, 23(12): 124703. **doi:** 10.1088/1674-1056/23/12/124703

Large-eddy simulations of a forced homogeneous isotropic turbulence with polymer additives

Wang Lu, Cai Wei-Hua, Li Feng-Chen

Chin. Phys. B . 2014, 23(3): 034701. **doi:** 10.1088/1674-1056/23/3/034701

Longitudinal and transverse structure functions in decaying nearly homogeneous and isotropic turbulence

Imtiaz Ahmad, Lu Zhi-Ming, Liu Yu-Lu

Chin. Phys. B . 2014, 23(1): 014701. **doi:** 10.1088/1674-1056/23/1/014701

Numerical study of heat-transfer in two- and quasi-two-dimensional Rayleigh–Bénard convection*

Zhen-Yuan Gao(高振源), Jia-Hui Luo(罗嘉辉), and Yun Bao(包芸)†

Department of Mechanics, Sun Yat-Sen University, Guangzhou 510275, *China*

(Received 12 April 2018; revised manuscript received 9 July 2018; published online 10 September 2018)

A detailed comparative numerical study between the two-dimensional (2D) and quasi-two-dimensional (quasi-2D) turbulent Rayleigh–Bénard (RB) convection on flow state, heat transfer, and thermal dissipation rate (TDR) is made. The Rayleigh number (*Ra*) in our simulations ranges up to 5×10^{10} and Prandtl number (*Pr*) is fixed to be 0.7. Our simulations are conducted on the Tianhe-2 supercomputer. We use an in-house code with high parallelization efficiency, based on the extended PDM–DNS scheme. The comparison shows that after a certain *Ra*, plumes with round shape, which is called the "temperature islands", develop and gradually dominate the flow field in the 2D case. On the other hand, in quasi-2D cases, plumes remain mushroom-like. This difference in morphology becomes more significant as *Ra* increases, as with the motion of plumes near the top and bottom plates. The exponents of the power-law relation between the Nusselt number (*Nu*) and *Ra* are 0.3 for both two cases, and the fitting pre-factors are 0.099 and 0.133 for 2D and quasi-2D respectively, indicating a clear difference in magnitude of the heat transfer rate between two cases. To understand this difference in the magnitude of *Nu*, we compare the vertical profile of the horizontally averaged TDR for both two cases. It is found that the profiles of both cases are nearly the same in the bulk, but they vary near boundaries. Comparing the bifurcation height $z_{\rm b}$ with the thermal boundary layer thickness δ_θ, it shows that $z_{\rm b}<\delta_\theta(3{\rm D})<\delta_\theta(2{\rm D})$ and all three heights obey a universal power-law relation $z\sim Ra^{-0.30}$. In order to quantify the difference further, we separate the domain by $z_{\rm b}$, i.e., define the area between two $z_{\rm b}$ (near top and bottom plates respectively) as the "mid region" and the rest as the "side region", and integrate TDR in corresponding regions. By comparing the integral it is found that most of the difference in TDR between two cases, which is connected to the heat transfer rate, occurs within the thermal boundary layers. We also compare the ratio of contributions to total heat transfer in BL–bulk separation and side–mid separation.

Keywords: Rayleigh–Bénard convection, Nusselt number, turbulence, thermal dissipation

PACS: 47.27.te **DOI:** 10.1088/1674-1056/27/10/104702

1. Introduction

Thermal convection exists widely in natural phenomena and industrial applications. Rayleigh–Bénard (RB) convection, which describes the convective motion of fluid in a closed sample heated from below and cooled from above, is one of its classical model systems.[1] Due to its complicated fluid motions with various coherent structures, it plays an important role in the researches on the heat transfer and turbulence mechanism.

The relation between the global heat transfer, indicated by the Nusselt number (*Nu*), and the control parameters of the system, i.e. Rayleigh number (*Ra*), and Prandtl number (*Pr*) is a hot issue in RB convection. Numbers of theoretical models have been proposed hitherto (see the review from Ahlers *et al.*[1] for details). Among them, the theory proposed by Grossmann and Lohse (GL)[2,3] is obviously the most successful one. Based on two exact equations connecting the thermal and viscous dissipation rate with *Nu*, GL theory decomposed these two dissipation rates into the boundary layer and bulk contributions. According to whether the boundary layer or bulk dominates the global heat transfer, the whole phase space can be divided into a few regimes. GL theory has successfully explained almost all experimental and numerical results up to the ultimate regime after updating its pre-factors by Stevens *et al.*[4] A great breakthrough has been made in experiments in recent years. The results for the *Ra* range $4\times10^{11}\leq Ra\leq2\times10^{14}$ at $Pr=0.8$ were reported by He *et al.*[5] Their results reveal that a transition in the power law relation between *Nu* and *Ra* comes up when $Ra>Ra_1^*(2\times10^{13})$. However, owing to the limits of experimental conditions like the lack of suitable working fluid, the reliable experimental result for high *Ra* is actually hard to obtain and the situation near the ultimate regime is still unclear.

With the development of computer hardware, the direct numerical simulations (DNS), which can simulate the idealized conditions exactly, becomes increasingly important in the research of RB turbulence. Huang *et al.*[6] investigated the effect of spatial confinement, i.e., aspect ratio Γ, through experiments and numerical simulations. They focused on convective cells with a rectangular shape and found that the *Nu* increases at a range of $\Gamma<1$, although the flow monotonically decreases

*Project supported by the National Natural Science Foundation of China (Grant Nos. 11772362 and 11452002) and the Special Scientific Research Fund for Super Computing in the Joint Fund of the National Natural Science Foundation of China and the People's Government of Guangdong Province (Phase II, Grant No. nsfc2015_570).

†Corresponding author. E-mail: stsby@mail.sysu.edu.cn

© 2018 Chinese Physical Society and IOP Publishing Ltd

with Γ. Schumacher *et al.*[7] extrapolated their DNS results to a larger Ra and concluded that the Ra^* of the ultimate region is about 10^{11} for $Pr = 0.021$. Actually, the computational resources required for simulations of RB convection with high Ra is huge since the meshes need to fully resolve the local Kolmogorov and Batchelor length scale of the flow, which decrease as Ra increases. For example, the simulation reported by Stevens *et al.*[8] for a $\Gamma = 0.5$ sample with $Ra = 2 \times 10^{12}$ and $Pr = 0.7$ was performed on a $2701 \times 671 \times 2501$ grid and took about 10^5 vectorial CPU hours on HLRS. However, compared with the three-dimensional (3D) case, the two-dimensional (2D) simulation needs much less CPU-time. This means that the 2D simulation can reach a higher Ra and a better resolution with the same numerical effort as the 3D simulation. Indeed, more and more results based on the 2D simulation have been reported over recent years. van der Poel *et al.*[9] investigated the local mean temperature profiles in the boundary layer and found the logarithmic behavior in regions where thermal plumes are emitted. Huang *et al.*[10] simulated a series of 2D samples and studied the mean temperature profiles near the bottom plate. Bao *et al.*[11] analyzed the effect of Pr in two dimensions for $0.05 \leq Pr \leq 20$ and $Ra = 10^{10}$.

There are lots of similarities between 2D and 3D convections, but significant differences also exist. Previously, a comparison work had been reported by van der Poel *et al.*[12] and it gave an overview on the system responses with data sets from numerical and experimental studies. Nevertheless, since all 3D results for high Ra were taken from experiments, a more detailed comparison on high Ra flow state and heat transfer is needed. Nowadays, we are able to achieve it by DNS.

In this paper, we show the DNS results for both 2D and quasi-2D cases over a range $10^9 \leq Ra \leq 5 \times 10^{10}$ at $Pt = 0.7$. We make a comparison on flow structures with the help of the flow visualization technique and provide a detailed study on Nu and the thermal dissipation rate (TDR). A characteristic height has been found and investigated with the thermal boundary layer.

2. Numerical methods

The simulations focus on a 2D square domain and a quasi-2D rectangular counterpart. We simulate the non-dimensional governing equations under the Boussinesq approximation as follows:

$$\nabla \cdot \boldsymbol{u} = 0, \tag{1}$$

$$\frac{D\boldsymbol{u}}{Dt} = -\nabla P + \frac{1}{\sqrt{Ra/Pr}}\nabla^2 \boldsymbol{u} + \theta \hat{z}, \tag{2}$$

$$\frac{D\theta}{Dt} = \frac{1}{\sqrt{Ra \cdot Pr}}\nabla^2 \theta, \tag{3}$$

where $\hat{z}$ is the vertical unit vector whose direction is opposite to gravity. $\boldsymbol{u}$, P, and θ represent the non-dimensional velocity, pressure, and temperature respectively. The normalization parameters we used to non-dimensionalize the governing equations are the height of domain H, the free-fall velocity $\sqrt{g\beta\Delta T H}$, and temperature difference between two horizontal plates ΔT. Three control parameters of the system, as previously mentioned, are defined as $Ra = g\beta\Delta T H^3/(\upsilon\kappa)$, $Pr = \upsilon/\kappa$, and $\Gamma = D/H$, where D is the length or the lateral width of the domain for the 2D and quasi-2D case respectively, g the acceleration of gravity, β the thermal expansion coefficient, υ the kinematic viscosity, and κ the thermal diffusivity.

The Parallel Direct Method of DNS (PDM–DNS), which is a highly efficient parallelization scheme, has been developed for 2D RB convection by Bao *et al.*[13] Compared to other DNS methods, the PDM–DNS method has two main advantages. One is that the Poisson equation of pressure is solved by introducing the parallel diagonal dominant (PDD) algorithm hence the amount of data needed to communicate decreases. The other is that the domain decomposition way is adjusted so that time-consuming all-to-all communication can be avoided. On such a basis, we extend the scheme to the quasi-2D situation and apply it to our simulation as well. The results prove that it also presents high efficiency and excellent scalability.

With the improved scheme, a series of 2D simulations are performed with Ra ranging from 10^8 to 5×10^{10} and $\Gamma = 1$. For comparisons, quasi-2D samples with Ra equal to 10^9, 10^{10}, and 5×10^{10} and $\Gamma = 1/4$ are simulated. All simulations are with Pr equal to 0.7 and conducted on the Tianhe-2 supercomputer. The boundary conditions are set as non-slip for velocity and impermeable for pressure on all walls. As for the boundary conditions for temperature, the sidewalls are adiabatic, and the top and bottom plates are those with fixed temperature $\theta_t = -0.5$ and $\theta_b = 0.5$ respectively.

To ensure the flow is fully resolved, high-resolution meshes with grid points refined near the horizontal plates were chosen, e.g., a 2048×2304 grid for the 2D case and a $1536 \times 192 \times 1728$ grid for the quais-2D case for $Ra = 5 \times 10^{10}$. According to the investigation by Stevens *et al.*,[14] the criteria of the resolution in grid design are to resolve the relevant scales, i.e., the Kolmogorov scale η_K and the Batchelor scale η_B. Moreover, the minimal number of grid points required for resolving the boundary layer is derived by Shishkina *et al.*[15] The meshes we used in the simulations fulfill both rules mentioned above. In addition, the time interval Δt we used is less than 1/1000 of the Kolmogorov time scale for all simulations, which means the temporal resolution is sufficient to catch the smallest time scale in turbulence. For all 2D simulations, the total time simulated is up to 1000 dimensionless time units, while that for quasi-2D simulations is 600 for $Ra = 10^9$, 300 for $Ra = 10^{10}$, and 260 for $Ra = 5 \times 10^{10}$.

3. Results and discussion

3.1. Flow structure

Figure 1 shows snapshots of instantaneous temperature fields for both 2D and quasi-2D cases. Three columns of the panels from left to right are for $Ra = 10^9$, $Ra = 10^{10}$, and $Ra = 5 \times 10^{10}$, respectively. Note that the colormap limit for all temperature snapshots in our study is set between $-0.1 \leq \theta \leq 0.1$ so that thermal plumes can be shown clearly. Additionally, a visualization method with transparency control is adapted to quasi-2D samples. By adjusting transparency according to the temperature value, it prevents the obstruction in view of the flow structure by that in front. It appears that, in contrast to the 3D case, the quasi-2D convection is more similar to the 2D one in the overall flow pattern. In the 3D case, the large-scale circulation (LSC) was found to be less pronounced and a certain portion of plumes would pass through the bulk directly from the center of the domain.[12] Whereas in both 2D and quasi-2D cases, a more pronounced single-roll LSC can be found. Under the drive of LSC, almost all plumes move to the opposite horizontal plate along the left or right sidewall. This is probably because in quasi-two dimensions the front and back walls limit the plumes on their motion.

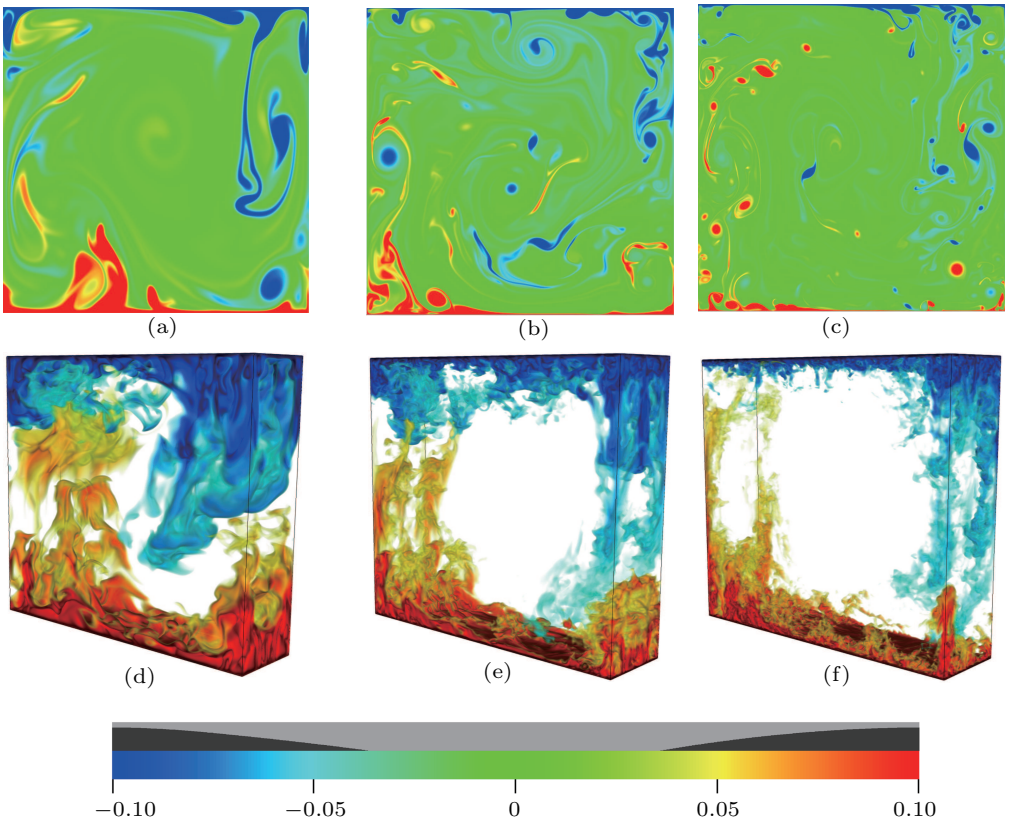


Fig. 1. (color online) Snapshots of instantaneous temperature fields for 2D (top panel) and quasi-2D case (bottom panel) at $Ra = 10^9$ [(a) and (d)], $Ra = 10^{10}$ [(b) and (e)], and $Ra = 5 \times 10^{10}$ [(c) and (f)]. The dark gray histogram over the colormap indicates the transparency of the corresponding temperature value in quasi-2D snapshots.

However, in terms of plume morphology, differences between both cases can be found and they grow with *Ra*. For lower *Ra*, both cases are dominated by mushroom-like plumes. The ribbon-like plumes, which are generated by the stretching of vortices, also exist in two dimensions. As *Ra* increases, it can be seen that the 2D plume morphology has changed and the flow is gradually dominated by the round shaped plumes, which we called the "temperature island". This type of plume is also observed in the work from van der Poel *et al.*[9] (see Fig. 1(a)). They are formed adjacent to the boundary layer and can move along with LSC until they are dissipated.[13] In the quasi-2D, plumes still keep mushroom-like while they become more and more incoherent, as shown in Figs. 1(d)–1(f).

By taking an average on the instantaneous flow data in the statistically steady state, the effects of transient structures can be averaged out and a time-averaged field, which reveals the large scale characteristics of the system, can be obtained. Figure 2 shows the time-averaged temperature field with corresponding streamlines for both 2D and quasi-2D cases. Specially, for the convenience of comparison, a spatial average along the lateral direction was made for the quasi-2D case. To ensure the results are statistically convergent, we collect data for at least 400 dimensionless time units for the 2D case and at least 100 for the quasi-2D case. Comparing both the top and bottom panels in Fig. 2, three main differences can be observed. First is the shape of LSC. The shape of 2D LSC is obviously round, rather than oval type, which was found in previous studies for *Ra* near 10^8.[16,17] However, in the

quasi-2D case, the shape of LSC is more like a short spindle. Second is the amount of corner rolls. The result reported by Zhang *et al.*[18] shows that several secondary rolls were found at four corners of the 2D domain for $Ra = 10^{10}$, $Pr = 5.3$. Analogously, we found that there are generally four corner rolls in two dimensions, while there are only two located at the plumes-impacting side of the domain in quasi-two dimensions. Third is the characteristics of plumes near sidewalls. It is seen that the regions with positive (negative) vertical velocity and higher (lower) temperature than the surrounding near sidewalls exist in both cases, which implies the condensation of plumes. Compared to those in the 2D case, the regions in the quasi-2D case are more transversally and longitudinally extended from the horizontal plates, as the figure shows. This suggests that the plumes near sidewalls behave more coherently and actively in the quasi-2D case.

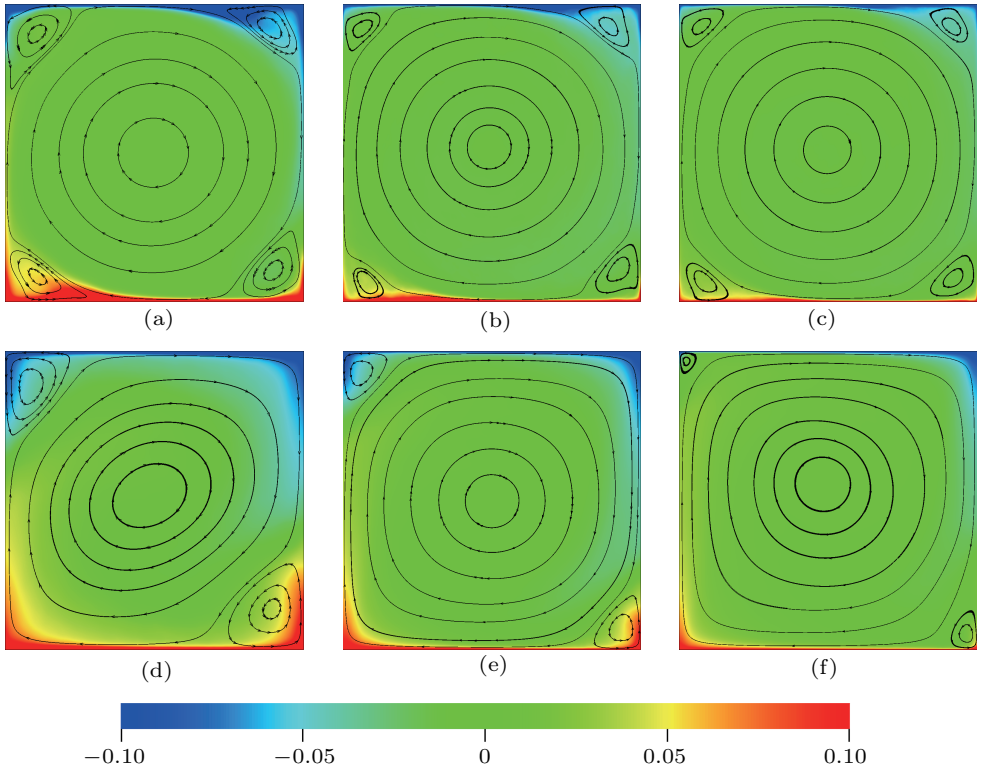


Fig. 2. (color online) Time-averaged temperature field and corresponding streamlines for 2D (top panel) and quasi-2D case (bottom panel) at $Ra = 10^9$ [(a) and (d)], $Ra = 10^{10}$ [(b) and (e)], and $Ra = 5 \times 10^{10}$ [(c) and (f)]. A spatial average along the lateral direction was made for the quasi-2D case.

In fact, the three differences mentioned above essentially can be concluded by one, which is the difference in moving paths of plumes. After detaching from the boundary layers, most 2D and quasi-2D plumes will move along the plate horizontally owing to the shear effects of LSC. The 2D plumes will be emitted at the position about $D/4$ away from sidewalls, which is understood as the "ejecting region".[9] However, the plumes in the quasi-2D case will keep moving and strike against the sidewalls directly. Then they condense near the corners and climb up along the sidewalls under the driving of LSC.

3.2. Nusselt number

In this subsection we come to the comparison of the Nusselt number Nu, which is defined as

$$Nu = \frac{Q}{\chi \Delta T / H}. \tag{4}$$

It represents the ratio between the convective heat transfer (Q) and the heat transferred only through conduction.[1] Here χ is the thermal conductivity of working fluid. In the present study, Nu is calculated by

$$Nu = \sqrt{Ra \cdot Pr}\langle u_z \theta \rangle_{V,t} - \langle \partial_z \theta \rangle_{V,t}, \tag{5}$$

where $\langle\,\rangle_{V,t}$ represents an average over the entire domain and time. Note that the total statistical times here are the same as those of the time-averaged flow field, which we investigated in the previous subsection. In the work from Huang *et al.*,[19] the time convergence was checked by comparing the time averages over the first and the last halves of each simulation. We check the Nu we obtained with this method and the relative errors of all cases are smaller than 1%.

Figure 3 shows the compensated $Nu/Ra^{0.3}$ as a function of Ra. The two-dimensional numerical results from Zhang *et al.*[18] and three-dimensional results from Stevens *et al.*[8] are also presented for reference. Comparing with 3D results, the quasi-2D points show a better agreement with the revised GL theory, which was indicated by the black solid line. This might be because the quasi-2D flow state, especially the state of LSC,

is less complex than that in a 3D cell whose $\Gamma = 1/2$. Stevens *et al.*[20] found that the LSC can be either in a single-roll state or in a double-roll state in such a cylindrical domain. This evolution in state, together with the Nu sensitiveness to the flow state at $Pr = 0.7$,[12] may influence the Nu.

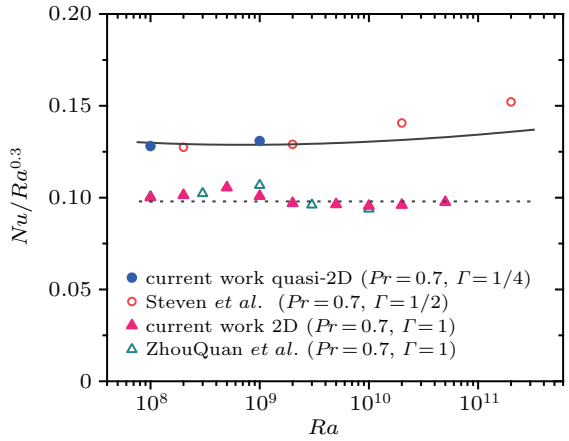


Fig. 3. (color online) Compensated $Nu/Ra^{0.3}$ as a function of Ra. Here all results are obtained by DNS. The 3D results from Stevens *et al.*[8] ($\Gamma = 1/2$) are indicated by the orange hollow circles and the present quasi-2D results are indicated by blue solid circles. Analogously, the 2D results from this work and Zhang *et al.*[18] are indicated by red solid triangles and green hollow triangles, respectively. The GL theory with updated pre-factors[4] is indicated by the black solid line. The dash line represents the best power-law fit of present 2D results.

The present 2D results also agree well with Zhang *et al.*[18] A clear difference can be found that the Nu in the 2D case is generally smaller than that in the quasi-2D case, although the power-law relation between Nu and Ra in both cases can be described well by a 0.30 exponent, which is consistent with the previous works for 3D situations.[1] We fit the data with the least-square method and the result gives a pre-factor 0.133 for quasi-two dimensions, which is within the range showed by Wagner *et al.*,[21] and a pre-factor 0.098 for two dimensions, which agrees with the result from Zhang *et al.*[18]

The comparison of Nu indicates that there are not only differences but also similarities between the heat transfer mechanism of 2D and quasi-2D RB convection. In the next subsections we will look for insights into this phenomenon through a detailed study on TDR.

3.3. Thermal dissipation rate

In a natural convective system, the heat energy carried by the fluid will be dissipated due to the thermal diffusion. The TDR is a quantity describing this process, whose dimensionless form is given by

$$\varepsilon_\theta(\boldsymbol{x},t) = \frac{1}{\sqrt{Ra \cdot Pr}} \sum_i \left[\frac{\partial \theta(\boldsymbol{x},t)}{\partial x_i} \right]. \tag{6}$$

According to the work reported by Shraiman *et al.*[22] and Siggia *et al.*,[23] for the closed RB system, there is an exact relation between the global averaged TDR $\langle \varepsilon_\theta(\boldsymbol{x},t) \rangle_{V,t}$ and Nu derived from the equations of motion with a dimensionless form as follows:

$$Nu = \sqrt{Ra \cdot Pr} \cdot \langle \varepsilon_\theta(\boldsymbol{x},t) \rangle_{V,t}. \tag{7}$$

Due to the close relation between the thermal dissipation rate and Nu, we next focus on the distribution of TDR.

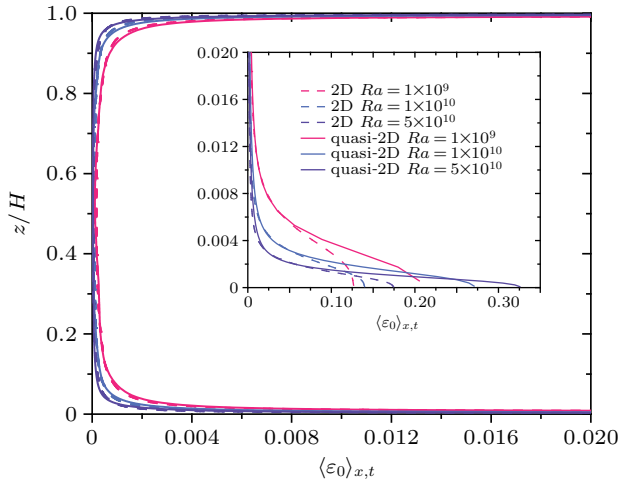


Fig. 4. (color online) Vertical profiles of averaged TDR. The inset is a local enlargement of the distribution near the bottom plate.

Figure 4 shows the vertical profiles of $\langle \varepsilon_\theta \rangle_{x,t}$. Note that $\langle\,\rangle_{x,t}$ represents an averaging in time and over a horizontal cross-section. It can be seen that for all Ra we focus on, the TDR curves of both cases collapse in the bulk. To be more specific, $\langle \varepsilon_\theta(\boldsymbol{x},t) \rangle_{x,t}$ of both the 2D and quasi-2D cases are negligible in the range $0.4 \le z \le 0.6$ and increases very slowly toward the top and bottom plates. However, at the region close to the horizontal plates, the trend changes. Taking the bottom half cell as an example, as the inset in Fig. 4 shows, $\langle \varepsilon_\theta \rangle_{x,t}$ increases rapidly in all cases, indicating that no matter in two dimensions or in quasi-two dimensions most of the thermal energy is dissipated near or within the thermal boundary layer. Furthermore, 2D and quasi-2D TDR curves still collapse until z reaches a critical height. Below this height, their curves separate and the difference grows as they approach the bottom plate. We call it bifurcation height and denote it by z_b. We observe that z_b reduces as Ra increases. In both cases TDR is maximized at the bottom surface. TDR distributions near the top plate are analogous. In summary, the results of $\langle \varepsilon_\theta \rangle_{x,t}$ imply that the difference between the 2D and quasi-2D cases in the heat transfer rate may originate from the region close to the horizontal plates. According to the experiments conducted in a cylindrical cell by Zhou *et al.*,[24] there are rod-like plumes within the thermal boundary layer and their number having a similar power-law relation with Ra as Nu. Such a kind of plume can also be found in the quasi-2D thermal boundary layer.[6] However, due to the lack of lateral direction, the rod-like plumes do not exist in the 2D case.

In the quasi-2D instantaneous flow near the bottom plate, several cold plumes impact the hot areas and then spread in all directions on the surface, just like a jet impinging on the flat-plate. As the plumes spread, they absorb heat from the horizontal plates efficiently, which sinks the local thermal boundary layer of the impacting region and induces a higher local heat transfer rate. Due to the limitation of space, the boundary of horizontal flow will meet, merge, and convolute. Finally they form the rod-like plumes and are also driven by LSC. It is noted that the boundary layer thickness in the region where the plumes formed is also thicker, indicating a lower local heat transfer rate.

From this point of view, the study in the characteristics of plumes near the bifurcation height may help to explain the difference in heat transfer rate between 2D and quasi-2D cases physically. This will be discussed in more detail in the future publication. In the present work, we mainly focus on the phenomenon and similarity among cases.

We first focus on the bifurcation height z_b, which indicates a region within which the thermal dissipation of the quasi-2D case is larger than the 2D cases. Since z_b is quite close to the horizontal plates and varies with Ra, it is analogous to the thickness of thermal boundary layers (δ_θ). We next compare z_b with δ_θ.

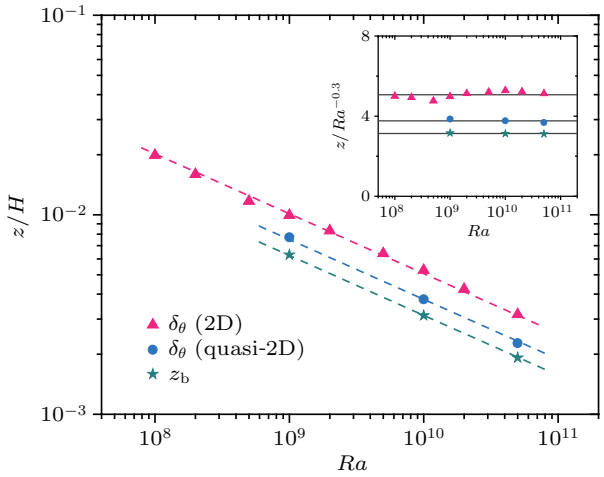


Fig. 5. (color online) Log-log plot of δ_θ and z_b as functions of Ra. The δ_θ in two- and quasi-two dimensions are indicated by red triangles and blue circles, respectively. The z_b are indicated by green stars. The dash lines represent the best power-law fits of corresponding cases. The inset is compensated $z/Ra^{-0.30}$ as a function of Ra.

According to Zhou *et al.*,[25] δ_θ is determined by the distance at which the tangent of the mean-temperature profile at the plate surface intersects the bulk temperature, which is zero in our present setup (see Fig. 4 in Zhou *et al.*[25]). δ_θ for all cases are shown in Fig. 5 together with zb in the log–log plot. In our simulations, δ_θ obeys the global estimation $H/(2Nu)$. In agreement with the fact that 2D cases yield smaller Nu than the quasi-2D cases, the thermal boundary layers in the quasi-2D case are thinner than that in the 2D case. As shown in Fig. 5, z_b is the lowest among the three heights, which indicates that the bifurcation phenomenon we observed above occurs within the thermal boundary layer. Furthermore, an experimental work whose setup covers the present parameter range has been reported by Belmonte *et al.*[26] Their results show an Ra scaling of thickness yields $\delta_\theta \sim Ra^{-0.29\pm0.01}$ for $Ra > 2\times10^7$. The best power-law fits of our data yield $\delta_\theta \sim Ra^{-0.299}$ for 2D cases and $\delta_\theta \sim Ra^{-0.308}$ for quasi-2D cases, which are consistent with the experiment. Moreover, the z_b scale as $Ra^{-0.303}$, suggesting that all three heights obey a universal power-law relation with an exponent being -0.30. The inset presents the compensated plot of three heights normalized by $Ra^{-0.30}$.

It should be noted that δ_θ is defined artificially. It is associated with the gradient of temperature near the horizontal plates and satisfy a reciprocal relation with Nu. Thus, it can also reflect the heat transfer in thermal convection. That is also why δ_θ in the 2D case is thicker than that in the quasi-2D case, as shown in Fig. 5. In contradiction, the bifurcation height z_b obtained from the vertical profiles of horizontally averaged TDR between both cases is a quantity that objectively exists. It reflects the difference in TDR of 2D and quasi-2D convections. Our result shows that z_b has a universal Ra-dependence with δ_θ, which reflects the heat transfer as discussed above. The smaller magnitude of zb comparing to the thermal boundary layer thickness of both 2D and quasi-2D cases reveals that the difference in TDR occurs within the thermal boundary layer.

In order to quantify the differences, the vertical profiles of TDR are integrated in separated regions. In previous studies, several separating methods are proposed. In the work reported by Kaczorowski and Wagner,[28] three regions, i.e., the bulk flow, the plumes or mixing layers, and the conductive sublayers were divided from the whole domain by two inflection points of the probability density function (PDF) of TDR. Besides that, the BL–bulk separation, which is also a key idea in GL theory, is no doubt the most classical method and widely discussed.[19,28,29] It is given by

$$\langle \varepsilon_\theta \rangle_{V,t} = \langle \varepsilon_\theta \rangle_{V_{\rm BL},t} + \langle \varepsilon_\theta \rangle_{V_{\rm bulk},t}, \tag{8}$$

where $V_{\rm BL}$ and $V_{\rm bulk}$ denote the BL and bulk regions, respectively. Hereafter $\langle\,\rangle_{V_*,t}$ represents the averaging over V_* and in time, multiplied by the volume ratio V_*/V. Analogously, we attempt to divide the domains into the side region and mid region by the bifurcation points, as figure 6(a) shows. The global thermal dissipation rate is separated into contributions from these two regions

$$\langle \varepsilon_\theta \rangle_{V,t} = \langle \varepsilon_\theta \rangle_{V_{\rm side},t} + \langle \varepsilon_\theta \rangle_{V_{\rm mid},t}. \tag{9}$$

The results of integration in corresponding regions are shown in a bidirectional histogram, see Fig. 6(b). The portion of the bar above the zero axis represents $\langle \varepsilon_\theta \rangle_{V_{\rm side},t}$ and

that below represents $\langle \varepsilon_\theta \rangle_{V_{\text{mid}},t}$, hence the whole bar represents the total TDR. The total TDR of two dimensions is generally smaller than quasi-two dimensions. In side regions, the region-averaged TDR in quasi-2D cases is obviously larger. As for the mid regions, both the 2D and quasi-2D cases yield close amounts of contributions in TDR. We further compare the contributions from side regions to the total difference in TDR between 2D and quasi-2D cases. The results show that over 94% of the TDR differences come from the side regions. Here we emphasize that according to the discussion about z_b above, the side regions are actually within the thermal boundary layer in both the 2D and quasi-2D cases. Namely, almost all differences in heat transfer between both cases originate from the thermal boundary layer.

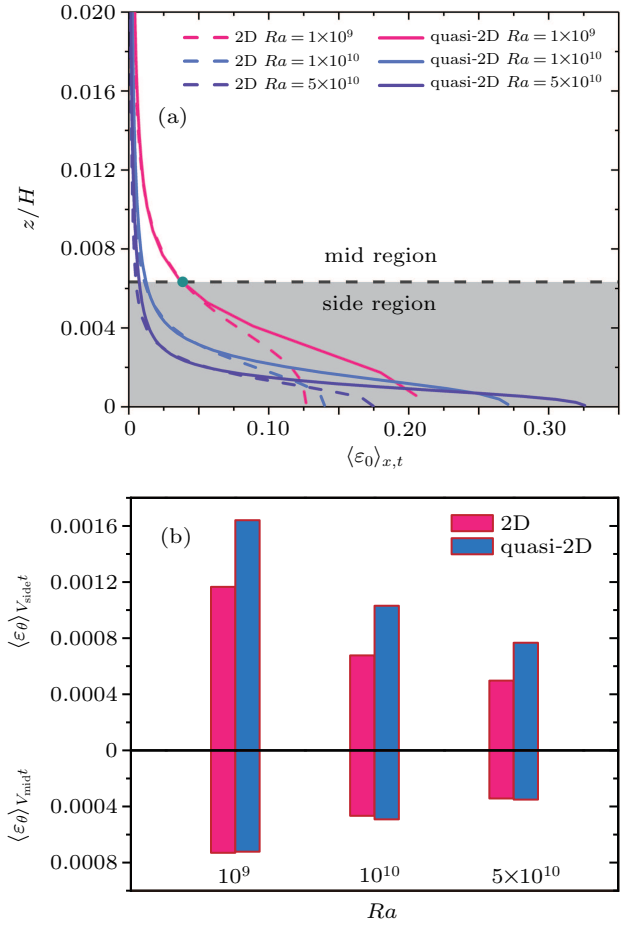


Fig. 6. (color online) (a) A sketch of the side–mid separation for $Ra = 10^9$. The bifurcation point is indicated by the cyan dot and the dash line represents the bifurcation height. (b) A bidirectional histogram of region-averaged TDR in two dimensions (red bars) and quasi-two dimensions (blue bars). The portions of bars that are above and below the zero axis represent $\langle \varepsilon_\theta \rangle_{V_{\text{side}},t}$ and $\langle \varepsilon_\theta \rangle_{V_{\text{mid}},t}$, respectively.

Next we compare the results of side–mid separation of TDR with BL–bulk separation. The previous studies reported by Verzicoo R *et al.*[28,29] suggest that for $Pr = 0.7$, the difference in contributions between BL and bulk regions grows with Ra up to 2×10^{11}, implying an increasing dominance of BL in thermal dissipation. However, as figure 7(a) shows, no matter whether in two dimensions or quasi-two dimensions, the ratio of contributions corresponding to these two regions barely changes with Ra, which is consistent with the results from Zhang *et al.*[19] Furthermore, the magnitude of contributions shows a certain consistency. In both the 2D and quasi-2D, the BL region contributes about 70%. In the quasi-2D case, the BL contribution is just slightly larger (about 2%) than the 2D case. It indicates that both cases are still dominated by the thermal boundary layer, which is consistent with the prediction of GL theory in the "classical regime".[2] Figure 7(b) shows the results from side–mid separation. It shows that for quasi-2D cases the results corresponding to two separating methods are very similar. As for the 2D cases, these two methods yield obviously different results.

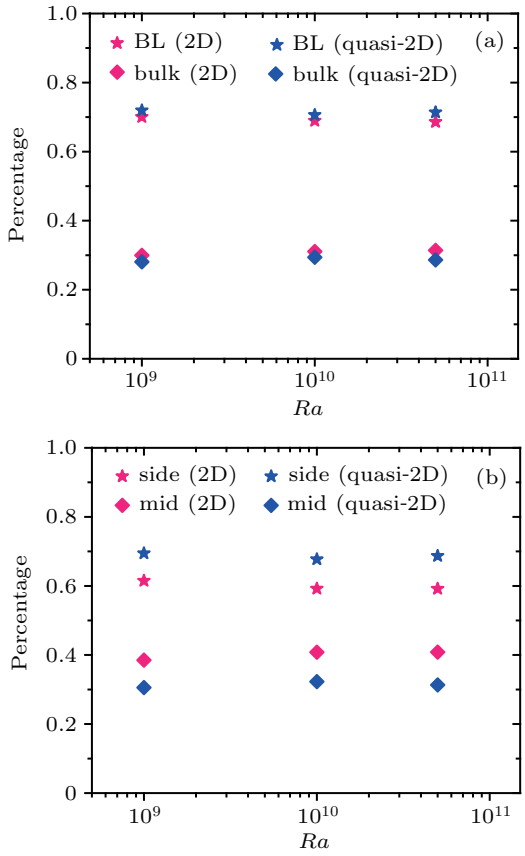


Fig. 7. (color online) The relative contributions of regions separated by BL–bulk (a) and side–mid (b) separations to total TDR as functions of Ra. All 2D cases are indicated by red markers while they are blue for quasi-2D cases. The contribution from BL or side regions is indicated by stars and that from bulk or mid regions is indicated by diamonds.

4. Conclusion

In this paper, we simulated 2D RB convection with Ra up to 5×10^{10} and $Pr = 0.7$, and quasi-2D convection with $Ra = 10^9$, 10^{10}, and 5×10^{10} by extended PDM–DNS, in a highly-efficient parallelization scheme. A detailed comparison between high Ra 2D and quasi-2D convections on the flow state, heat transfer, and thermal dissipation is conducted. We summarize the major findings and list them as follows:

(i) As *Ra* increases, the difference in flow state between both cases grows. The 2D flow state is gradually dominated by round-shaped plumes called "temperature islands", while the quasi-2D plumes still keep mushroom-like but become incoherent. The motions of plumes near the horizontal plates are also different. The 2D plumes leave the plates from the position about $D/4$ away from sidewalls, i.e., the "ejecting region",[10] earlier than its quasi-2D counterpart, which impact the sidewalls directly.

(ii) It is found that the quasi-2D *Nu* agrees well with the GL theory.[4] No matter in two or quasi-two dimensions, the power-law relation between *Nu* and *Ra* can be described well by a 0.30 exponent. However, a clear difference in magnitude can be found. The fitted pre-factors are 0.099 for the 2D case and 0.133 for the quasi-2D case.

(iii) The vertical distributions of horizontally averaged TDR in both convections are all most the same in the bulk, while the curves separate near the horizontal plates and the quasi-2D TDR is larger subsequently. The bifurcation height is compared with the thickness of thermal boundary layers. We find that $z_{\rm b} < \delta_\theta(3{\rm D}) < \delta_\theta(2{\rm D})$ and all the three heights obey a unified power-law relation of *Ra* with an exponent -0.30.

(iv) Furthermore, the profiles of TDR have been integrated in regions separated by side–mid separation according to the bifurcation height. The result confirms that the difference in heat transfer between the 2D case and quasi-2D case mainly comes from the side region, which is within the thermal boundary layer. We compare the side–mid separation with BL–bulk separation. It shows that in both cases the contributions hardly vary with *Ra*. Their magnitude shows a certain consistency, implying that both cases are still dominated by the thermal boundary layers. Under side–mid separation, the quasi-2D contributions are similar to those in BL–bulk separation, while the 2D counterparts become more equal.

Acknowledgment

The authors thank Huang S D and Ding G Y for their useful discussions and advice.

References

[1] Ahlers G, Grossmann S and Lohse D 2009 *Rev. Mod. Phys.* **81** 503
[2] Grossmann S and Lohse D 2000 *J. Fluid Mech.* **407** 27
[3] Grossmann S and Lohse D 2001 *Phys. Rev. Lett.* **86** 3316
[4] Stevens R J A M, Van Der Poel E P, Grossmann S and Lohse D 2013 *J. Fluid Mech.* **730** 295
[5] He X Z, Funfschilling D, Nobach H, Bodenschatz E and Ahlers G 2012 *Phys. Rev. Lett.* **108** 024502
[6] Huang S D, Kaczorowski M, Ni R and Xia K Q 2013 *Phys. Rev. Lett.* **110** 104501
[7] Schumacher J, Bandaru V, Pandey A and Scheel J D 2016 *Phys. Rev. Fluids* **1** 84402
[8] Stevens R J A M, Lohse D and Verzicco R 2011 *J. Fluid Mech.* **688** 31
[9] Van Der Poel E P, Ostilla-Mico R, Verzicco R, Grossmann S and Lohse D 2015 *Phys. Rev. Lett.* **115** 154501
[10] Huang M J and Bao Y 2017 *Sci. Sin. Phys. Mech. Astron.* **47** 064701 (in Chinese)
[11] Bao Y, Gao Z Y and Ye M X 2018 *Acta Phys. Sin.* **61** 014701 (in Chinese)
[12] Van Der Poel E P, Steven R J A M and Lohse D 2013 *J. Fluid Mech.* **736** 177
[13] Bao Y, Luo J H and Ye M X 2017 *J. Mech.* **34** 159
[14] Stevens R J A M, Verzicco R and Lohse D 2010 *J. Fluid Mech.* **643** 495
[15] Shishkina O, Jam S R, Grossmann S and Lohse D 2010 *New J. Phys.* **12** 075022
[16] Van Der Poel E P, Stevens R J A M and Lohse D 2010 *Phys. Rev. E* **84** 45303
[17] Huang M J, Bao Y 2016 *Acta Phys. Sin.* **20** 204702 (in Chinese)
[18] Zhang Y, Zhou Q and Sun C 2017 *J. Fluid Mech.* **814** 165
[19] Huang Y X and Zhou Q 2013 *J. Fluid Mech.* **737** R3
[20] Stevens R J A M, Clercx H J H and Lohse D 2011 *Phys. Fluids* **23** 095110
[21] Wagner S, Shishkina O and Wagner C 2012 *J. Fluid Mech.* **697** 336
[22] Shraiman B I and Siggia E D 1990 *Phys. Rev. A* **42** 3650
[23] Siggia E D 1994 *Ann. Rev. Fluid Mech.* **26** 137
[24] Zhou Q and Xia K Q 2010 *New J. Phys.* **12** 075006
[25] Zhou Q and Xia K Q 2013 *J. Fluid Mech.* **721** 199
[26] Belmonte A, Tilgner A and Libchaber A 1994 *Phys. Rev. E* **50** 269
[27] Kaczorowski M and Wagner C 2009 *J. Fluid Mech.* **618** 89
[28] Verzicco R 2003 *Eur. Phys. J. B* **35** 133
[29] Verzicco R and Camussi R 2003 *J. Fluid Mech.* **477** 19